

# Isotopic transient analysis of ammonia synthesis over Ru/MgO catalysts promoted by cesium, barium, or lanthanum

Stacey E. Siporin and Robert J. Davis \*

*Department of Chemical Engineering, University of Virginia, Charlottesville, VA 22904-4741, USA*

Received 8 September 2003; revised 21 October 2003; accepted 22 October 2003

## Abstract

The global and intrinsic kinetics of ammonia synthesis over ruthenium supported on MgO ( $\sim 2$  wt% Ru) and promoted with Cs, Ba, or La were examined at 3 atm and various dihydrogen pressures with steady-state and isotopic transient measurements. Steady-state, global measurements revealed that Cs–Ru/MgO was strongly inhibited by dihydrogen whereas Ba–Ru/MgO and La–Ru/MgO were weakly inhibited by the reactant. However, the isotopic transient measurements showed that the intrinsic turnover frequency was a weak positive function of dihydrogen pressure regardless of the added base. Promotion by these compounds appeared to be electronic in nature because their presence increased the intrinsic turnover frequency of an active site, with Cs being the most effective. However, the coverage of nitrogen-containing intermediates was greater on Ba- and La-promoted catalysts than on Cs–Ru/MgO at 673 K and stoichiometric conditions. Therefore, the global activity of a promoted catalyst is a competition between inhibition by dihydrogen and enhancement of dinitrogen dissociation. Furthermore, promotion with Cs, Ba, and La introduced a new and highly active class of sites to the Ru/MgO system.

© 2003 Elsevier Inc. All rights reserved.

**Keywords:** Magnesium oxide; Promotion of ruthenium; Isotopic transient analysis; Ammonia synthesis; Cesium; Barium; Lanthanum; Hydrogen inhibition

## 1. Introduction

Ammonia synthesis is traditionally carried out over a multipromoted iron catalyst at high temperatures and pressures. Consequently, a more active catalyst that reduces the energy consumption is highly desired. Ruthenium-based materials are thought to be the next generation catalysts for ammonia synthesis since they exhibit higher specific activity, less inhibition by ammonia, and greater tolerance of poisons [1]. The relatively high cost of Ru requires a high dispersion of the metal on a suitable support, thus exposing a significant fraction of the atoms to the surface.

The first industrial use of a Ru-based ammonia synthesis catalyst was in the early 1990s in the Ocelot Ammonia Plant in British Columbia [1]. A carbon-supported Ru catalyst allowed for less severe operating conditions compared to those normally associated with the iron catalyst, resulting in lower capital costs and a reduction of energy consumption of 1 million BTU/ton ammonia produced [2]. However, ruthenium is known to catalyze carbon gasification [3,4]. Uncertainty

with regard to catalyst lifetime may inhibit widespread utilization of Ru catalysts in ammonia plants [5]. Thus, current research in the field also includes studies of nonreducible oxides as potential supports for Ru. In this work we have chosen to support Ru on MgO. In addition to the support, another critical component of an active Ru catalyst is a basic promoter such as an alkali or alkaline-earth metal oxide or hydroxide.

Basic promoters have been shown to increase the global activity of Ru catalysts [6–39]. The effectiveness of promoters generally scales with basicity, with alkali metal oxides or hydroxides usually being the best. It was therefore interesting to find that alkaline-earth and lanthanide promoters such as Ba and La oxides or hydroxides can be effective promoters for Ru [6,8–12,14,18–22,24,25,27,28,30–40]. Promotion of ammonia synthesis catalysts by Ba is not restricted to Ru-based materials. The activity of cobalt and iron–cobalt alloy catalysts is significantly enhanced with Ba promoters [41].

Zeng and co-workers studied barium promotion of Ru on activated carbon [42]. The active form of the Ba promoter is thought to be BaO rather than Ba(OH)<sub>2</sub> under ammonia synthesis conditions due to the unfavorable equilibrium concentration of Ba(OH)<sub>2</sub> [42]. In contrast, a Cs promoter is

\* Corresponding author.

E-mail address: [rjd4f@virginia.edu](mailto:rjd4f@virginia.edu) (R.J. Davis).

expected to be in the hydroxide form under ammonia synthesis conditions [8,42].

The role of alkali, alkaline-earth, and rare earth promoters on Ru ammonia synthesis catalysts is still not understood. One plausible explanation is that the basic promoter or support facilitates the dissociative adsorption of dinitrogen by donating electrons to surface Ru atoms or changing the induced dipole upon  $N_2$  adsorption [9,10,19,28,29,40,43,44]. Alternatively, others suggest that promoters reduce the surface coverage of nitrogen-containing species, freeing sites for dinitrogen dissociation [9,43].

Cesium has been postulated to be an electronic promoter that increases the intrinsic activity of the Ru catalyst [9,10,25,28,30,32]. Results from isotopic transient analysis, temperature-programmed reaction, and X-ray photoelectron spectroscopy of Cs-promoted Ru catalysts on carbon and MgO support that proposition. However, Ba has been claimed by some researchers to be a structural promoter [9,18,25,32]. This type of promoter is one that increases the concentration of active sites. From results of temperature-programmed reaction of adsorbed nitrogen atoms in the presence of dihydrogen on Ru/MgO, Szmigiel et al. hypothesized that a Ba promoter increases the concentration of  $B_5$  surface sites which are claimed to be active for ammonia synthesis [9]. Furthermore, for the Co catalyst supported on activated carbon, Ba was claimed to increase the number of active sites [41]. In contrast, Hansen and co-workers used in situ high-resolution transmission electron microscopy of Ba-promoted Ru supported on boron nitride to show that Ba does not alter the morphology of Ru and must therefore be an electronic promoter [31,40]. In addition, McClaine and Davis used isotopic transient analysis to suggest that Ba promotion of Ru/BaX is electronic in nature [28]. Furthermore, Rossetti et al. determined through XPS that alkaline-earth promoters for Ru/C are electronic in nature [30]. Evidently, promotion of ammonia synthesis catalysts by bases is not yet understood.

Typically, Ru catalysts are strongly inhibited by dihydrogen, with the order of reaction often approaching  $-1$ , suggesting that the catalysts should be operated under the less thermodynamically favorable nonstoichiometric conditions [11,26]. A supported Ru catalyst that is less inhibited by  $H_2$  is therefore highly desirable. Lanthanides used both as supports and promoters have been shown to decrease the inhibition by dihydrogen [19–24,27]. For example, lanthanum promotion of Ru on zeolitic supports nearly eliminates dihydrogen inhibition during ammonia synthesis at a total pressure of 20 atm. An alkaline-earth promoter such as Ba has also demonstrated a similar reduction in  $H_2$  inhibition on Co and Co–Fe alloy catalysts [41].

The goal of this work is to clarify the role of Cs, Ba, and La promotion of Ru/MgO and to understand why the choice of promoter affects the dihydrogen reaction order since dinitrogen dissociation is the generally thought to be the rate determining step. Steady-state isotopic transient analysis (SSITKA) will be used to help answer these questions. An

examination of both global and intrinsic kinetic parameters and their changes with varying dihydrogen partial pressures will be addressed here.

Ammonia synthesis catalysts should be studied under working conditions (i.e., elevated temperatures and pressures) because the reaction is highly structure sensitive [45] and the surface structure can be dependent on the reaction conditions. Unfortunately, a direct comparison of the effect of promoters (i.e., alkali metal, alkaline-earth, and lanthanide oxide or hydroxides) on the intrinsic kinetic behavior of Ru under reaction conditions has been minimal. In our previous work, Cs-promoted Ru/MgO was studied under reaction conditions using SSITKA [10].

Ammonia synthesis catalyzed by both Fe [46] and Ru [10, 28,47] has been studied previously with SSITKA. This technique is very powerful because it allows for the characterization of a catalyst surface under working conditions. The SSITKA experiment is carried out under steady-state conditions following a step change in the isotopic content of a reactant (dinitrogen in this case). The pressure, temperature, total flow rate, and product compositions are constant during this step change. A mass spectrometer is used to record the transient responses of isotopically labeled products (ammonia). Therefore, in the absence of isotopic mass effects, the steady state is not altered during the step change. From the transient response, the surface coverage of adsorbed reaction intermediates that lead to ammonia and the residence time of adsorbed reaction intermediates ( $NH_x = N, NH, NH_2$ , and  $NH_3$ ) can be determined. Recently, Shannon and Goodwin reviewed the theory underlying this technique [48]. Because of significant isotopic mass effects during  $H_2/D_2$  switches, the coverage of H was not determined. However, through the use of  $^{14}N_2/^{15}N_2$  switches, the coverage of  $NH_x$  species on the surface during steady-state reaction was determined.

## 2. Experimental methods

### 2.1. Catalyst preparation

The preparation method was similar to that used previously [10–12]. The starting material, magnesia (Ube Industries,  $42\text{ m}^2\text{ g}^{-1}$ ) was mixed with approximately 2 wt% Ru in the form of  $Ru_3(CO)_{12}$  (Aldrich, 99%), dissolved in THF. The THF was removed by evaporation. The resulting  $Ru_3(CO)_{12}/MgO$  sample was then heated in vacuum at a rate of  $0.5\text{ K min}^{-1}$  to 723 K and held at temperature for 2 h (final pressure  $< 10^{-5}$  Torr). After cooling, the sample was then heated in  $20\text{ ml min}^{-1}$   $H_2$  (palladium purified, Matheson 8371V) at  $1\text{ K min}^{-1}$  to 723 K, held at that temperature for 1 h, evacuated, and cooled under vacuum (final pressure  $< 10^{-5}$  Torr) before exposing to air. The promoter was then added in a 1:1 atomic ratio with ruthenium by impregnation of Ru/MgO with aqueous cesium nitrate (Aldrich, 99.999%), barium nitrate (Aldrich, 99.999%), or lanthanum nitrate (Aldrich, 99.99%). Lastly, each sample was heated to

723 K in flowing  $N_2$  ( $50 \text{ ml min}^{-1}$ , 99.999%, BOC gases, further purified with OMI-2 filter from Supelco) at a heating rate of  $1 \text{ K min}^{-1}$ . All catalysts (Cs–Ru/MgO, Ba–Ru/MgO, La–Ru/MgO and the unpromoted catalyst Ru/MgO) were crushed and sieved between 250 and  $425 \mu\text{m}$ .

## 2.2. Adsorption of dihydrogen

The fraction of Ru exposed on each of the catalysts was determined by chemisorption of dihydrogen (Eastman Chemical Company). Before dihydrogen adsorption, a sample was heated under vacuum at  $2 \text{ K min}^{-1}$  to 673 K, reduced in flowing dihydrogen for 30 min, evacuated, and then cooled under vacuum. The chemisorption was measured at 308 K. Turnover frequencies based on hydrogen chemisorption ( $\text{TOF}_{\text{global}}$ ) and surface coverages of nitrogen containing species ( $\theta_{\text{NH}_x}$ ) were based on surface Ru atoms counted by total hydrogen chemisorption (extrapolated to zero pressure) assuming a  $H/\text{Ru}_{\text{surf}}$  ratio of unity.

## 2.3. Isotopic transient measurements during ammonia synthesis

Approximately 0.270 g of catalyst were loaded into a 4-mm inside diameter quartz tubular reactor. Quartz wool was used to hold the sample in place. The catalyst was heated to 723 K at  $2 \text{ K min}^{-1}$  under flowing dihydrogen (99.999%, BOC gases; palladium purified, Matheson 8371V) and dinitrogen (99.999%, BOC gases, further purified with OMI-2 filter) in a stoichiometric ratio, a flow rate of  $40 \text{ ml min}^{-1}$ , and 3 atm total pressure. The catalyst was held at 723 K for 2 h before cooling to the desired temperature.

A schematic representation of the SSITKA apparatus can be found in prior work [10,28]. A step change in isotopically labeled dinitrogen was accomplished by switching between a stream of normal dinitrogen ( $^{14}\text{N}_2/\text{Ar}$ ) and  $^{15}\text{N}_2$  (Isotec, 98+%, further purified with OMI-2 filter). The normal dinitrogen (BOC gases, further purified with OMI-2 filter) contained 1.06% Ar in order to monitor the gas-phase holdup of the system. However, this amount of Ar was not large enough to disturb the steady state of the system. Dihydrogen (and He when needed) was added after the pneumatically controlled switch. Gases were supplied via mass-flow controllers of all reactants and backpressure regulators ensured that all reactant streams and vent lines were maintained at 3 atm. Helium (99.999%, BOC gases, further purified with OMI-2 filter) was used to balance the flow rate in the vent lines.

A Balzers-Pfeiffer Prisma 200 amu mass spectrometer monitored the concentrations of  $^{14}\text{NH}_2$ ,  $^{14}\text{NH}_3$ ,  $^{15}\text{NH}_3$ ,  $^{14}\text{N}_2$ ,  $^{15}\text{N}_2$ , and Ar ( $m/e = 16, 17, 18, 28, 30$ , and 40, respectively) continuously. The concentration of  $^{15}\text{NH}_3$  ( $m/e = 18$ ) was used to calculate the transient responses. The lines from the reactor effluent to the mass spectrometer as well as the mass spectrometer housing were heated to

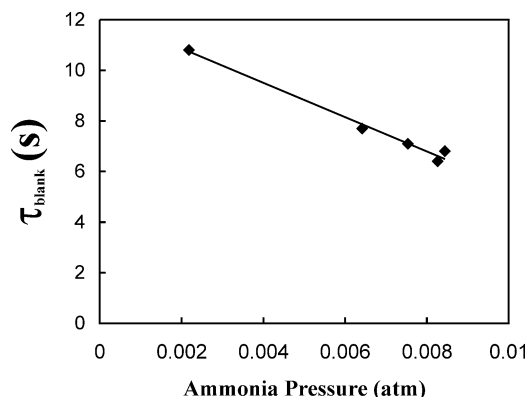


Fig. 1. Characteristic  $\tau$  of the blank reactor system ( $\tau_{\text{blank}}$ ).

443 K. Multiple forward switches ( $^{14}\text{N}_2/\text{Ar} \rightarrow ^{15}\text{N}_2$ ) and reverse switches ( $^{15}\text{N}_2 \rightarrow ^{14}\text{N}_2/\text{Ar}$ ) were recorded under each condition. Operating the catalyst at thermodynamic equilibrium allowed the mass spectrometer to be calibrated for ammonia in each run.

A small amount of ammonia adsorption in the lines to the mass spectrometer was evident after monitoring the ammonia concentration following a switch without any catalyst present in the reactor. The mean residence time of ammonia in the system itself therefore was recorded as  $\tau_{\text{blank}}$ . This adsorption can cause an overestimation of the residence time of nitrogen containing species,  $\tau_{\text{cat}}$ , that is associated with the catalyst surface. In order to ensure a correct estimation of  $\tau_{\text{cat}}$ , the residence time without catalyst present ( $\tau_{\text{blank}}$ ) was subtracted from the experimentally determined  $\tau$ . Fig. 1 shows  $\tau_{\text{blank}}$  as a function of ammonia pressure. The regression line was used to estimate  $\tau_{\text{blank}}$  at other ammonia pressures.

Each catalyst was evaluated at 673 K, 3 atm, a total flow rate of  $40 \text{ ml min}^{-1}$ , and  $\text{N}_2:\text{H}_2 = 1:3$ . To determine the effect of dihydrogen pressure on intrinsic kinetics, the promoted catalysts were evaluated at 623 K, 3 atm, a total flow rate of  $40 \text{ ml min}^{-1}$ , a dinitrogen partial pressure of 0.75 atm, and ratios of  $\text{N}_2:\text{H}_2:\text{He}$  between 1:3:0 and 1:0.33:2.67. In addition, the effect of ammonia readsorption on the catalyst particles was evaluated for the La-promoted catalyst by recording the isotopic transient responses at total flow rates of 20, 40, and  $60 \text{ ml min}^{-1}$  (3 atm, 673 K, and  $\text{N}_2:\text{H}_2 = 1:3$ ).

## 3. Results

According to results in Table 1, addition of promoters lowered the amount of dihydrogen uptake, which could result from a partial covering of the metal surface with the promoter or sintering of Ru into larger particles. At this time we cannot ascertain which is the likely cause. However, Zupanc and co-workers have also studied the hydrogen chemisorption on Ru/MgO and Cs–Ru/MgO with temperature-programmed desorption, volumetric chemisorp-

Table 1  
Properties of MgO-supported Ru catalysts

Catalyst	Ru (wt%)	Promoter (wt%)	Mol promoter/mol Ru	H/Ru <sub>tot</sub>
Ru/MgO	1.66	—	—	0.77
Cs–Ru/MgO	1.64	2.04	0.95	0.52
Ba–Ru/MgO	1.40	2.39	1.26	0.15
La–Ru/MgO	1.59	2.11	0.97	0.17

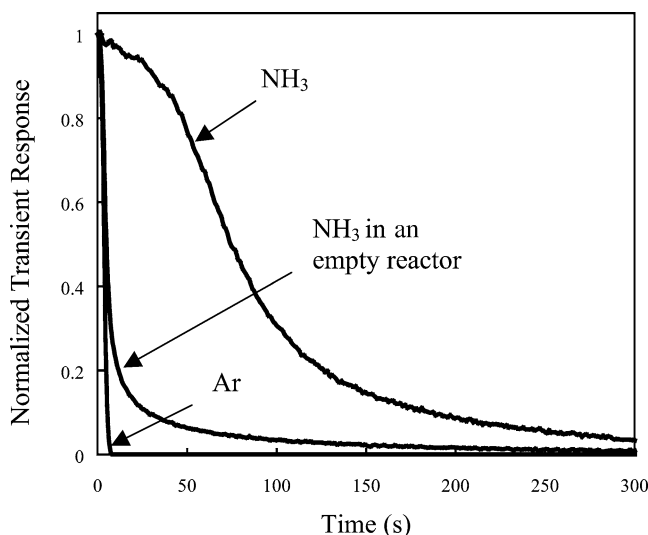


Fig. 2. Typical normalized isotopic transient responses of ammonia and Ar as a function of time for La–Ru/MgO at 623 K, 3 atm, 40 ml min<sup>−1</sup>, and N<sub>2</sub>:H<sub>2</sub> = 2:1.

tion, and microkinetic modeling. They concluded that the Cs promoter blocks low-coordinated defect-like sites, which suppresses a fast nonactivated path for adsorption [49]. Rosowski et al. have also used TEM and XRD of these catalysts to show that the addition of the CsNO<sub>3</sub> promoter increased the Ru particle size from 2 nm to up to 10 nm [26]. Nevertheless, the results from dihydrogen chemisorption were used to calculate the coverage of nitrogen-containing species,  $\theta_{\text{NH}_x}$ , as well as the global turnover frequency (TOF<sub>global</sub>) under each condition.

A typical set of isotopic transients for ammonia following a switch between <sup>14</sup>N<sub>2</sub>/Ar and <sup>15</sup>N<sub>2</sub> can be found in Fig. 2. In addition, this figure shows the Ar transient and the NH<sub>3</sub> transient in an empty reactor. The average residence time of surface intermediates leading to ammonia ( $\tau_{\text{cat}}$ ) is calculated by integrating the area between the normalized transients,

$$\tau_{\text{cat}} = \int_0^{\infty} [F_{\text{cat}}^{14\text{NH}_3}(t) - F_{\text{blank}}^{14\text{NH}_3}(t)] dt, \quad (1)$$

$$\tau_{\text{cat}} = \int_0^{\infty} [1 - F_{\text{cat}}^{15\text{NH}_3}(t) - F_{\text{blank}}^{15\text{NH}_3}(t)] dt, \quad (2)$$

where,  $F_{\text{cat}}^{15\text{NH}_3}$  and  $F_{\text{blank}}^{14\text{NH}_3}$  are the normalized transient responses for <sup>15</sup>NH<sub>3</sub> and the blank transient that was

collected following a step change from NH<sub>3</sub>/N<sub>2</sub>/H<sub>2</sub> to N<sub>2</sub>/H<sub>2</sub> under similar conditions without catalyst present, respectively. Both the <sup>14</sup>NH<sub>3</sub> transient response in an empty reactor and the Ar transient response were significantly quicker than the <sup>15</sup>NH<sub>3</sub> transient response in the presence of catalyst. It should be noted that  $\tau_{\text{cat}}$  does not depend explicitly on the overall steady-state rate nor the value of surface coverage of intermediates. The number of surface intermediates per gram of catalyst,  $N_{\text{NH}_3}$ , was calculated using the following steady-state mass balance,

$$N_{\text{NH}_3} = \tau_{\text{cat}} R_{\text{NH}_3}, \quad (3)$$

where  $R_{\text{NH}_3}$  is the steady-state rate of ammonia synthesis per gram of catalyst. The coverage of nitrogen-containing species on the surface of the catalyst can then be calculated by dividing  $N_{\text{NH}_3}$  by the amount of total hydrogen chemisorbed per gram of catalyst. Finally, the intrinsic turnover frequency is defined as

$$\text{TOF}_{\text{intr}} = 1/\tau_{\text{cat}}. \quad (4)$$

This relationship assumes that ammonia synthesis can be described by the expression

$$\text{rate} = k\theta_{\text{NH}_x}, \quad (5)$$

where  $\theta_{\text{NH}_x}$  is the coverage of nitrogen containing species ( $x = 0\text{--}3$ ) and  $k$  is a pseudo-first-order rate constant [48].

It is possible that ammonia can readsorb on catalytically active and inactive sites before leaving the reactor, which will cause an overestimation of  $\tau_{\text{cat}}$  and  $\theta_{\text{NH}_x}$ . However, the global rate of ammonia synthesis,  $R_{\text{NH}_3}$ , is unaffected by the overestimation. In our previous work, we showed that for a similarly prepared Cs-promoted Ru/MgO catalyst the effect of ammonia readsorption was negligible [10]. However, ammonia readsorption on a zeolite-supported Ru catalyst was severe [28]. Therefore, the influence of ammonia readsorption was reexamined in this study. The total flow rate was varied between 20 and 60 ml min<sup>−1</sup> over the La-promoted catalyst at 673 K, 3 atm, and stoichiometric conditions. The results are summarized in Table 2 and in Fig. 3. Increasing the total flow rate by a factor of three changed  $\tau_{\text{cat}}$  by less than 20%. Therefore, the effect of ammonia readsorption on the lifetime of surface intermediates was minimal. Therefore

Table 2  
SSITKA Results at 673 K, 3 atm, and N<sub>2</sub>:H<sub>2</sub> = 1:3

Catalyst	Total flow rate (ml min <sup>−1</sup> )	$P_{\text{NH}_3}$ (atm)	TOF <sub>global</sub> (10 <sup>−4</sup> s <sup>−1</sup> )	$\tau_{\text{cat}}$ (s)	$\theta_{\text{NH}_x}$ <sup>a</sup>	TOF <sub>intr</sub> <sup>b</sup> (10 <sup>−4</sup> s <sup>−1</sup> )
Ru/MgO	40	0.0026	13.6	410 ± 2.3	0.056	244
Cs–Ru/MgO	40	0.0095	64.1	8 ± 2.6	0.051	1250
Ba–Ru/MgO	40	0.0039	54.2	20 ± 2.8	0.108	500
La–Ru/MgO	40	0.0052	75.3	19 ± 0.4	0.143	526
La–Ru/MgO	20	0.0088	63.7	23 ± 2.1	0.146	435
La–Ru/MgO	60	0.0040	86.8	19 ± 1.2	0.165	526

<sup>a</sup> Based on total hydrogen chemisorption.

<sup>b</sup> TOF<sub>intr</sub> = 1/ $\tau_{\text{cat}}$ .

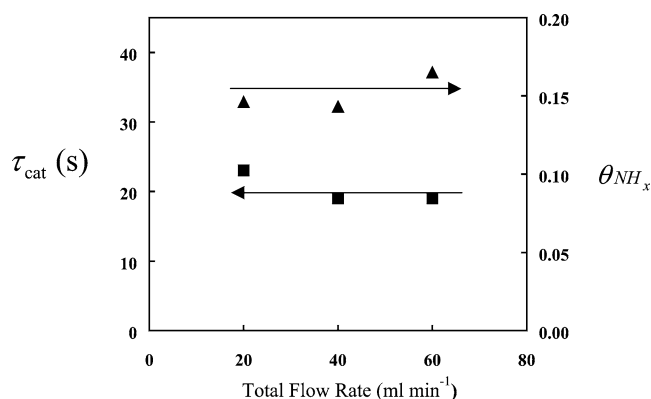


Fig. 3. Effect of total flow rate on the intrinsic kinetics of La-Ru/MgO.

it is assumed that  $\tau_{\text{cat}}$  is a good estimate of the residence time of nitrogen-containing species on all catalyst samples studied here.

Under conditions close to equilibrium, reaction reversibility (i.e.,  $\text{N}_2 + 3\text{H}_2 \rightarrow 2\text{NH}_3 \rightarrow \text{N}_2 + 3\text{H}_2$ ) can also lead to an overestimation of the residence time of nitrogen-containing species. To avoid this complication, all intrinsic kinetic parameters were determined under conditions that were at least 70% from equilibrium.

The global turnover frequency,  $\text{TOF}_{\text{global}}$ , determined at 3 atm, 673 K, and stoichiometric conditions is reported for each catalyst in Table 2. This turnover frequency was based on the ammonia partial pressure at the reactor outlet and the amount of sites on the catalyst that was titrated by dihydrogen chemisorption. Comparison of the  $\text{TOF}_{\text{global}}$  determined at  $40 \text{ ml min}^{-1}$  shows that addition of Cs, Ba, or La to Ru/MgO increases the rate by at least a factor of 4. The La-promoted catalyst exhibited the highest global turnover frequency under these conditions. However, the  $\text{TOF}_{\text{global}}$  of the Cs and Ba-promoted catalysts was only 17 and 39% less, respectively.

The intrinsic turnover frequency,  $\text{TOF}_{\text{intr}}$ , determined by SSITKA revealed a different trend. The Cs-promoted catalyst was the most active of the series; it was 10 times greater than the Ru/MgO catalyst. Promotion with Ba and La resulted in a catalyst with a  $\text{TOF}_{\text{intr}}$  less than half that of Cs-Ru/MgO, but superior to unpromoted Ru/MgO. In all cases,  $\text{TOF}_{\text{global}}$  was significantly lower than  $\text{TOF}_{\text{intr}}$ .

The coverage of nitrogen-containing species that lead to ammonia was quite small on all of the catalysts (0.05–0.14). Although the intrinsic turnover frequency of Ba-Ru/MgO and La-Ru/MgO was lower than Cs-Ru/MgO,  $\theta_{\text{NH}_x}$  was greater by a factor of 2 or 3 on those catalysts.

The order of reaction with respect to dihydrogen was examined for each of the promoted catalysts. Table 3 summarizes the conditions used and the results obtained for the experiments performed at various partial pressures of  $\text{H}_2$ . Fig. 4 shows the  $\text{TOF}_{\text{global}}$  as a function of dihydrogen pressure at 623 K and  $40 \text{ ml min}^{-1}$ . The cesium-promoted catalyst was strongly inhibited by dihydrogen, with an order of reaction ( $\alpha_{\text{H}_2}$ ) equal to  $-0.87$ , which is in excellent agree-

Table 3

Effect of  $\text{H}_2$  pressure on the global and intrinsic kinetics at 623 K, 3 atm, and  $40 \text{ ml min}^{-1}$

Catalyst	$P_{\text{H}_2}^a$ (atm)	$P_{\text{NH}_3}$ (atm)	$\text{TOF}_{\text{global}}^b$ ( $10^{-4} \text{ s}^{-1}$ )	$\tau_{\text{cat}}$ (s)	$\theta_{\text{NH}_x}^b$	$\text{TOF}_{\text{intr}}^c$ ( $10^{-4} \text{ s}^{-1}$ )
Cs-Ru/MgO <sup>d</sup>	1.00	0.0060	76.2	$14 \pm 1.1$	0.107	714
Cs-Ru/MgO <sup>d</sup>	1.50	0.0050	63.5	$14 \pm 3.2$	0.089	714
Cs-Ru/MgO <sup>d</sup>	2.25	0.0030	38.1	$12 \pm 0.9$	0.046	833
Ba-Ru/MgO	0.38	0.0015	28.0	$48 \pm 3.5$	0.135	208
Ba-Ru/MgO	0.75	0.0016	29.9	$42 \pm 1.8$	0.126	238
Ba-Ru/MgO	1.50	0.001	18.7	$41 \pm 3.7$	0.077	244
Ba-Ru/MgO	2.25	0.0008	15.0	$38 \pm 3.1$	0.057	263
La-Ru/MgO	0.38	0.0010	14.5	$64 \pm 1.6$	0.093	156
La-Ru/MgO	0.75	0.0010	14.5	$53 \pm 7.0$	0.077	189
La-Ru/MgO	2.25	0.0009	13.0	$39 \pm 1.5$	0.051	256

<sup>a</sup> Initial dihydrogen partial pressure with an initial dinitrogen partial pressure of 0.75 atm.

<sup>b</sup> Based on total hydrogen chemisorption.

<sup>c</sup>  $\text{TOF}_{\text{intr}} = 1/\tau_{\text{cat}}$ .

<sup>d</sup> 0.098 g of catalyst was used for this study.

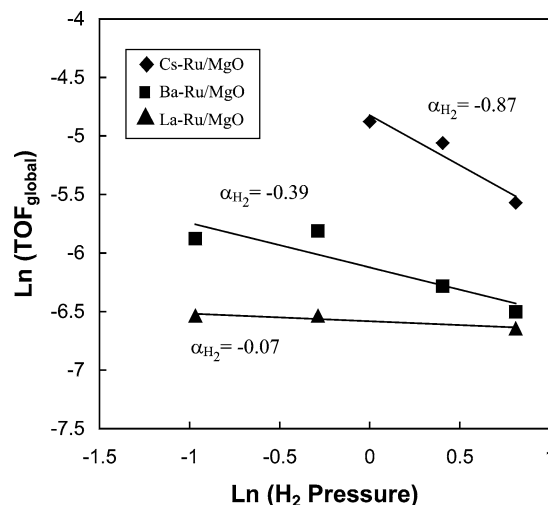


Fig. 4. Global turnover frequency ( $\text{TOF}_{\text{global}}$ ) as a function of dihydrogen partial pressure at 3 atm, 623 K, and  $40 \text{ ml min}^{-1}$ .

ment with the literature [11,26]. However, promotion by Ba or La decreased the inhibition by  $\text{H}_2$ . Fig. 5 illustrates the effect of dihydrogen partial pressure on  $\text{TOF}_{\text{intr}}$  and surface coverage of  $\text{NH}_x$  species. The partial pressure of  $\text{H}_2$  was changed by at least a factor of 2.25 while holding the partial pressure of  $\text{N}_2$  and the total flow rate constant. The order of reaction with respect to  $\text{H}_2$  is small and slightly positive for all promoters. Competitive adsorption of  $\text{H}_2$  accounts for the inhibition observed in the global rate measurements. Indeed, the coverage of  $\text{NH}_x$  decreased by more than a factor of 2 over the pressure range studied.

#### 4. Discussion

Through experiments and theoretical calculations, Dahl and co-workers have shown that steps in the Ru(0001) sur-

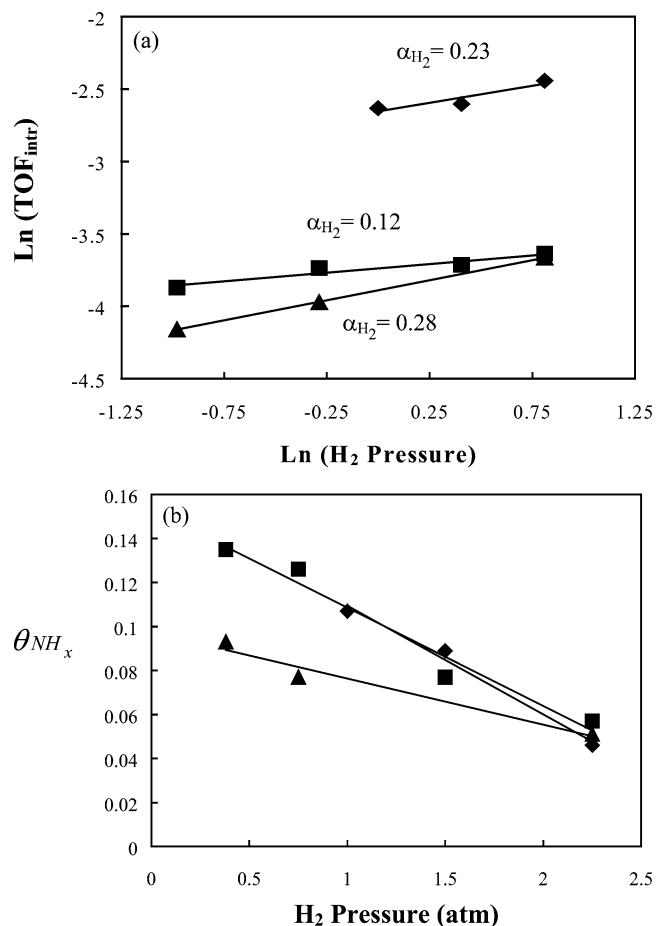


Fig. 5. Intrinsic kinetic parameters as a function of hydrogen partial pressure at 3 atm, 623 K, and  $40 \text{ ml min}^{-1}$  where (a) is the intrinsic turnover frequency, (b) is the coverage of nitrogen-containing species,  $\alpha_{\text{H}_2}$  is the order of reaction with respect to dihydrogen for Cs–Ru/MgO (◆), Ba–Ru/MgO (■), and La–Ru/MgO (▲).

face are the location of sites that dissociate  $\text{N}_2$  [43,50,51]. Furthermore, they suggest that this type of site is a so-called  $\text{B}_5$  site [51]. The  $\text{B}_5$ -type site is a cluster of five atoms at low coordinated edge sites. Very small clusters of metal atoms will have very few of these sites; in fact a spherical cluster size of at least 1 nm is needed to form any of the  $\text{B}_5$ -type sites [51]. The number of  $\text{B}_5$  sites per gram of catalyst is maximized on spherical particles of about 2 nm [51].

Typically, the number of active sites for a metal-catalyzed reaction is estimated to be the number of exposed metal atoms. Dihydrogen or carbon monoxide chemisorption is frequently used to count the number of exposed metal atoms. Once the number of metal sites is estimated, a global turnover frequency can then be calculated. However, ammonia synthesis over Ru is very sensitive to surface structure. Each exposed Ru atom is not necessarily an active site since a specific ensemble of Ru atoms is required to dissociate dinitrogen. Therefore, chemisorption of  $\text{H}_2$  or CO may overestimate the number of active sites, resulting in lower calculated turnover frequency.

Steady-state isotopic transient analysis is a very useful technique for studying structure-sensitive reactions such as ammonia synthesis since the catalyst can be tested under working conditions (i.e., elevated temperatures and pressures). Here, no assumption about the number of active sites is required to calculate a turnover frequency.

The  $\text{TOF}_{\text{intr}}$  evaluated in this study is a measure of the turnover of nitrogen-containing intermediates on the surface. McClaine and Davis measured a  $\text{TOF}_{\text{intr}}$  of  $0.141 \text{ s}^{-1}$  and a coverage of nitrogen-containing species of 0.051 for a similar Cs–Ru/MgO catalyst (average Ru particle size of 1.0 nm) at 673 K, 3 atm, and stoichiometric conditions [10]. In current work, a Cs–Ru/MgO catalyst was tested under identical conditions and the results are in good agreement (see Table 2).

The  $\text{TOF}_{\text{intr}}$  of Cs–Ru/MgO in this work was five times as great as Ru/MgO, while promotion of Ru/MgO with Ba or La resulted in a catalyst that was intrinsically twice as active as the unpromoted Ru/MgO catalyst. The Cs promoter resulted in the most intrinsically active catalyst, which is consistent with the idea that catalytic activity parallels promoter basicity. Since the intrinsic turnover frequency is a good measure of the turnover of nitrogen on the surface, an increase in  $\text{TOF}_{\text{intr}}$  with addition of promoters suggests that the Cs promoter is electronic in nature. McClaine and Davis also concluded from isotopic transient studies that Cs promotion of Ru/MgO is electronic in nature [10].

The global activity of Ru/MgO in this work was more than an order of magnitude greater than that on Ru/SiO<sub>2</sub> studied earlier under identical conditions [10]. Magnesium oxide is a solid base, and therefore acts both as a support for the ruthenium and as a basic promoter. Therefore, the activity of this catalyst was expected to be significantly higher than a Ru/SiO<sub>2</sub> catalyst.

Under all conditions examined in this study and regardless of the promoter, the intrinsic turnover frequency ( $\text{TOF}_{\text{intr}}$ ) was much larger than the global turnover frequency ( $\text{TOF}_{\text{global}}$ ). Although SSITKA provides an intrinsic rate of turnover of an active surface, the number density of active sites cannot be evaluated directly. Competitive adsorption of  $\text{H}_2$  lowers the surface coverage of  $\text{NH}_x$  species under reaction conditions.

The coverage of nitrogen-containing species was significantly larger on the Ba- and La-promoted catalysts compared to Cs–Ru/MgO. There appears to be a trade-off between  $\text{NH}_x$  coverage and intrinsic activity of the promoted samples. The Cs-promoted catalyst was intrinsically the most active but had the lowest coverage of nitrogen-containing intermediates. Since barium- and lanthanum-promoted samples had higher coverages of nitrogen-containing intermediates, their global turnover frequencies were similar to that of the Cs-promoted catalyst. The consequence of using Cs as a promoter is its effect on the inhibition by dihydrogen. Apparently, the electronic promotion of the surface that results in more effective dissociation of  $\text{N}_2$  also causes a stronger interaction with hydrogen. The activity of base-promoted

Ru/MgO catalysts is a consequence of competitive adsorption of  $N_2$  and  $H_2$ . We are currently performing a detailed kinetic analysis of high-pressure reaction studies to formulate a microkinetic model. Preliminary results indicate that while Cs lowers the barrier for  $N_2$  dissociation, it also increases the enthalpy of hydrogen adsorption, which is consistent with the results presented here.

Koningsberger and co-workers have recently observed a similar trade-off for alkane hydrogenolysis over supported Pt [52]. They concluded that the more basic the support, the larger the enthalpy of dihydrogen adsorption (larger the coverage of H) and the more negative the reaction order in dihydrogen. They suggest that the change in reaction order is a result of a change in the hydrogen-binding geometry with different supports [52].

Since the rate-determining step in ammonia synthesis is often considered to be the dissociation of dinitrogen, all other steps in the reaction sequence involving adsorbed nitrogen might be at quasi-equilibrium. Thus, the intrinsic activation energy determined from SSITKA is somewhat related to the barrier for dissociative chemisorption of  $N_2$ . Two point activation energies for each of the promoted catalysts were determined using  $TOF_{intr}$  at 3 atm, stoichiometric conditions, and  $40 \text{ ml min}^{-1}$  as presented in Tables 2 and 3. The activation energies for Cs–Ru/MgO, Ba–Ru/MgO, and La–Ru/MgO are 28, 45, and  $50 \text{ kJ mol}^{-1}$ , respectively. The lowest activation energy is associated with the most intrinsically active catalyst, which is consistent with Cs being the best electronic promoter of the series. Hinrichsen et al. used temperature-programmed desorption (TPD) and the  $N_2$  isotopic exchange reaction ( $^{14}N^{14}N + ^{15}N^{15}N \leftrightarrow 2^{14}N^{15}N$ ) on Cs–Ru/MgO to determine an activation energy for dinitrogen dissociation of  $33 \text{ kJ mol}^{-1}$  [17]. Our results are in good agreement with their findings.

The heterogeneity of the surface-active sites (in this case only ones occupied by nitrogen containing species) can be determined by plotting the logarithm of the normalized transient response as a function of time [48]. The abscissa in Fig. 6 is the time it takes  $^{14}N$  to replace  $^{15}N$  and is not the time on stream. There is no evidence for catalyst deactivation in this study. The presence of concavity in the plot suggests that the transient response cannot be estimated with one exponential curve (Eq. (1)), but rather multiple exponential curves. This behavior is indicative of multiple types of sites, operating in parallel. However, the sites are operating in series if the curve is S shaped. The S-shaped curve results because the reactants must first get to a relatively inactive site (where the transient response does not decrease very much with time) and then migrate to another more active site (as evidence from a rapid decrease in the normalized transient with time) where the reactants turn to products more readily [48].

The normalized transient response curves for each of the Ru/MgO catalysts studied here are shown in Fig. 6 (673 K, 3 atm,  $40 \text{ ml min}^{-1}$ , and stoichiometric conditions). The curve for the Ru/MgO catalyst is S shaped, indicating two

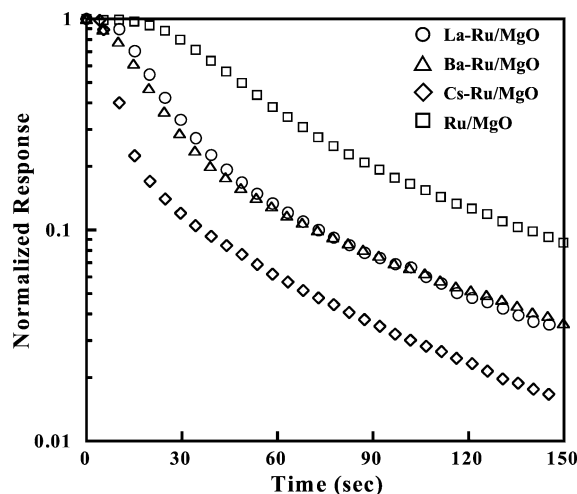


Fig. 6. Normalized transients of  $^{15}NH_3$  at 673 K, 3 atm,  $N_2:H_2 = 1:3$  and  $40 \text{ ml min}^{-1}$  for Cs-, Ba-, and La-promoted Ru/MgO as well as the unpromoted catalyst (Ru/MgO). For clarity, not all points are shown.

sites operating in series. After an initial delay in the response, the curve is characteristic of a single exponential decay. However, the response curves for the Cs-, Ba-, and La-promoted catalysts are all concave. Evidently, each catalyst contained at least two different types of sites, one highly active site (represented by large negative slope) and one relatively inactive site (represented by small negative slope). The observed catalysis was dominated by the most active sites. The slopes for the promoted catalysts at long times were similar to that of the unpromoted Ru/MgO catalyst, suggesting that these were of the same type. Apparently, base promotion was necessary to create the highly active sites on the catalysts.

Nwalor and Goodwin determined that promotion of Ru/SiO<sub>2</sub> with K created a new additional type of site that was very active [47]. McClaine and Davis suggested that both the Cs–Ru/MgO and Ru/SiO<sub>2</sub> catalysts contained a relatively uniform site distribution [10]. Therefore, the heterogeneity of active sites appears to be system dependent.

## 5. Conclusions

Steady-state isotopic transient analysis revealed that promotion by Cs, Ba, and La oxides or hydroxides is likely to be electronic in nature. In addition, promotion of Ru by bases is a trade-off between strong dihydrogen inhibition and low activation barrier for dinitrogen dissociation, with more of a balance observed with the Ba- and La-promoted Ru catalysts. Furthermore, basic promoters create a new class of highly active sites on the Ru/MgO catalyst.

## Acknowledgments

This work was supported by the National Science Foundation (Grant CTS-9729812) and the Department of Energy (Basic Energy Sciences, Grant DE-FG02-95ER14549).

The authors acknowledge Dr. John Monnier from Eastman Chemical Company for dihydrogen chemisorption and Ru elemental analysis.

## References

- [1] K. Aika, K. Tamaru, in: A. Nielsen (Ed.), *Ammonia Catalysis and Manufacture*, vol. 1, Springer, Berlin, 1995, p. 104.
- [2] Chementator, *Chem. Engr.* 3 (1993) 19.
- [3] P.J. Goethel, R.T. Yang, *J. Catal.* 111 (1988) 220.
- [4] R. Baker, *Carbon* 24 (1986) 715.
- [5] C.J.H. Jacobsen, *Chem. Commun.* (2000) 1057.
- [6] S. Murata, K.-I. Aika, *J. Catal.* 136 (1992) 118.
- [7] K. Aika, A. Ohya, A. Ozaki, Y. Inoue, I. Yasumori, *J. Catal.* 92 (1985) 305.
- [8] K.-I. Aika, T. Takano, S.J. Murata, *J. Catal.* 136 (1992) 126.
- [9] D. Szmigiel, H. Bielawa, M. Kurtz, O. Hinrichsen, M. Muhler, W. Rarog, S. Jodzis, Z. Kowalczyk, L. Znak, J. Zielinski, *J. Catal.* 205 (2002) 205.
- [10] B.C. McClaine, R.J. Davis, *J. Catal.* 210 (2002) 387.
- [11] T. Becue, R.J. Davis, J.M. Garces, *J. Catal.* 179 (1998) 129.
- [12] B.C. McClaine, T. Becue, C. Lock, R.J. Davis, *J. Mol. Catal. A Chem.* 163 (2000) 105.
- [13] K. Aika, M. Kumasaka, T. Oma, O. Kato, H. Matsuda, N. Watanabe, K. Yamazaki, A. Ozaki, T. Onishi, *Appl. Catal.* 28 (1986) 57.
- [14] C.T. Fishel, R.J. Davis, J.M. Garces, *J. Catal.* 163 (1996) 148.
- [15] Y. Izumi, M. Hoshikawa, K. Aika, *Bull. Chem. Soc. Jpn.* 67 (1994) 3191.
- [16] O. Hinrichsen, F. Rosowski, M. Muhler, G. Ertl, *Chem. Eng. Sci.* 51 (1996) 1683.
- [17] O. Hinrichsen, F. Rosowski, A. Hornung, M. Muhler, G. Ertl, *J. Catal.* 165 (1997) 33.
- [18] H. Bielawa, O. Hinrichsen, A. Birkner, M. Muhler, *Angew. Chem. Int. Ed.* 40 (6) (2001) 1061.
- [19] Y. Niwa, K.-I. Aika, *Res. Chem. Int.* 24 (5) (1998) 593.
- [20] Y. Niwa, K.-I. Aika, *J. Catal.* 162 (1996) 138.
- [21] S. Murata, K.-I. Aika, T. Onishi, *Chem. Lett.* (1990) 1067.
- [22] Y. Niwa, K.-I. Aika, *Chem. Lett.* (1996) 3.
- [23] Y. Izumi, Y. Iwata, K.-I. Aika, *J. Phys. Chem.* 100 (1996) 9421.
- [24] Y. Kadowaki, K.-I. Aika, *J. Catal.* 161 (1996) 178.
- [25] W. Rarog, Z. Kowalczyk, J. Sentek, D. Skladanowski, J. Zielinski, *Catal. Lett.* 68 (2000) 163.
- [26] F. Rosowski, A. Hornung, O. Hinrichsen, D. Herein, M. Muhler, G. Ertl, *Appl. Catal. A* 151 (1997) 443.
- [27] S.E. Siporin, B.C. McClaine, S.L. Anderson, R.J. Davis, *Catal. Lett.* 81 (2002) 265.
- [28] B.C. McClaine, R.J. Davis, *J. Catal.* 211 (2002) 379.
- [29] S. Dahl, J. Sehested, C.J.H. Jacobsen, E. Tornqvist, I. Chorkendorff, *J. Catal.* 192 (2000) 391.
- [30] I. Rossetti, N. Pernicone, L. Forni, *Appl. Catal.* 208 (2001) 271.
- [31] T.W. Hansen, J.B. Wagner, P.L. Hansen, S. Dahl, H. Topsøe, C.J.H. Jacobsen, *Science* 294 (2001) 1508.
- [32] W. Rarog-Pilecka, D. Szmigiel, Z. Kowalczyk, S. Jodzis, J. Zielinski, *J. Catal.* 218 (2003) 465.
- [33] K.-I. Aika, T. Kawahara, S. Murata, T. Onishi, *Bull. Chem. Soc. Jpn.* 63 (1990) 1221.
- [34] Z. Zhong, K.-I. Aika, *Inorg. Chim. Acta* 280 (1998) 183.
- [35] Z. Zhong, K.-I. Aika, *Chem. Commun.* (1997) 1223.
- [36] Z. Zhong, K.-I. Aika, *J. Catal.* 173 (1998) 535.
- [37] L. Forni, D. Molinari, I. Rossetti, N. Pernicone, *Appl. Catal. A* 185 (1999) 269.
- [38] C. Liang, Z. Wei, Q. Xin, C. Li, *Appl. Catal. A* 208 (2001) 193.
- [39] Z. Kowalczyk, S. Jodzis, W. Rarog, J. Zieliński, J. Pielaszek, *Appl. Catal. A* 173 (1998) 153.
- [40] T.W. Hansen, P.L. Hansen, S. Dahl, C.J.H. Jacobsen, *Catal. Lett.* 84 (2002) 7.
- [41] S. Hagen, R. Barfod, R. Fehrmann, C.J.H. Jacobsen, H.T. Teunissen, I. Chorkendorff, *J. Catal.* 214 (2003) 327.
- [42] H.S. Zeng, K. Inazu, K.I. Aika, *J. Catal.* 211 (2002) 33.
- [43] S. Dahl, A. Logadottir, C.J.H. Jacobsen, J.K. Nørskov, *Appl. Catal. A* 222 (2001) 19.
- [44] J.J. Mortensen, Y. Morikawa, B. Hammer, J.K. Nørskov, *J. Catal.* 169 (1997) 33.
- [45] S. Dahl, E. Tornqvist, I. Chorkendorff, *J. Catal.* 192 (2000) 381.
- [46] J.U. Nwalor, J.G. Goodwin Jr., P. Biloen, *J. Catal.* 117 (1989) 121.
- [47] J.U. Nwalor, J.G. Goodwin Jr., *Top. Catal.* 1 (1994) 285.
- [48] S.L. Shannon, J.G. Goodwin Jr., *Chem. Rev.* 95 (1995) 677.
- [49] C. Zupanc, A. Hornung, O. Hinrichsen, M. Muhler, *J. Catal.* 209 (2002) 501.
- [50] S. Dahl, A. Logadottir, R.C. Egeberg, J.H. Larsen, I. Chorkendorff, E. Tornqvist, J.K. Nørskov, *Phys. Rev. Lett.* 83 (1999) 1814.
- [51] C.J.H. Jacobsen, S. Dahl, P.L. Hansen, E. Tornqvist, L. Jensen, H. Topsøe, D.V. Prip, P.B. Moenshaug, I. Chorkendorff, *J. Mol. Catal. A* 163 (2000) 19.
- [52] D.C. Koningsberger, M.K. Oudenhuijzen, J. deGraaf, J.A. van Bokhoven, D.E. Ramaker, *J. Catal.* 216 (2003) 178.